ARTEMIS

Advanced Reusable Transport for Exploration Missions

Gateway-Based Human Lunar Surface Access

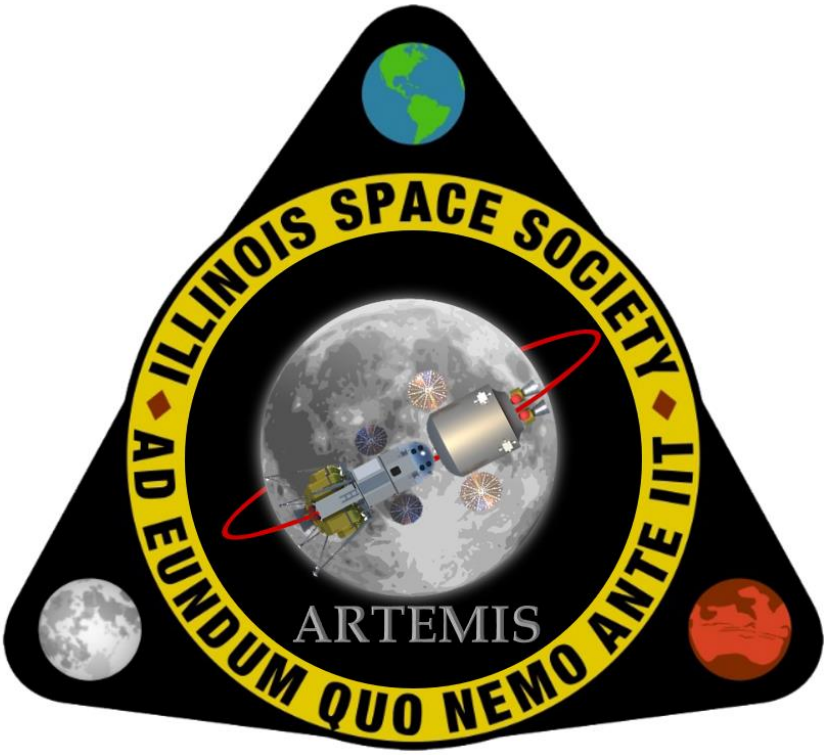

University of Illinois at Urbana-Champaign

Illinois Space Society

May 30, 2019

Project Manager: Linyi Hou

Daniel Engel, Brian Hardy, Jacob Hawkins, Erika Jarosch, Rahil Makadia, Megha Natarajan, Harsh Patel, Haoyun Qiu, Peter Sakkos, Edward Taylor, Jessica Yoon

Faculty Advisors: Koki Ho, Ph.D. and Michael Lembeck, Ph.D.

Table of Contents

1 Introduction 1

1.1 Motivation and Background 1

1.2 Scope of the Study 1

1.3 Design Summary 1

2 Concept of Operations 1

2.1 Mission Profile 1

2.2 Staging Method 2

2.3 Mission Modes and Surface Operations 3

3 Structures 3

3.1 Orbiter 3

3.2 Lander 3

3.3 Drop Tanks 5

4 Vehicle Subsystems 5

4.1 Power Systems 5

4.2 Telemetry, Tracking, and Command 5

4.3 Micrometeorite and Orbital Debris (MMOD) and Radiation Shielding 6

4.4 Thermal Control 6

4.5 Propulsion 7

4.6 Reaction Control System 8

5 Environmental Control and Life Support Systems (ECLSS) 8

5.1 Atmosphere Baselines and Regulations 9

5.2 Waste Management 9

5.3 Consumables and Habitation 9

5.4 Crew Radiation Mitigation 10

5.5 Acoustic Analysis 10

5.6 Spacesuits 10

6 Gateway Operations 11

6.1 Resupply and Refueling 11

6.2 Gateway Effects 11

6.3 Uncrewed Operations 11

7 Design, Development, and Testing 12

7.1 Design and Development 12

7.2 Procurement, Manufacturing, and Testing 12

7.3 Launch and Validation 12

8 Business Plan 13

9 Extended Capabilities **13**
10 Risk Assessment Matrix **14**
Appendix A: Calculations and Tables **16**
Appendix B: Theme Compliance Matrix **23**
Appendix C: References **24**

1 Introduction

The Illinois Space Society proposes the Advanced Reusable Transport for Exploration Missions (ARTEMIS), a Gateway-based reusable architecture for sustainable human lunar surface access.

1.1 Motivation and Background

NASA's lunar Gateway is designed to enable human access to the lunar surface and ultimately support crewed missions to Mars. In recent months, Vice President Mike Pence directed NASA to return humans to the surface of the Moon by 2024, and a pre-solicitation was issued by NASA for commercial companies to study and prototype reusable landers for this very purpose [1]. Concurrently, as interest has risen in returning humans to the Moon, ongoing studies have also uncovered the potential for future missions to leverage in-situ resource utilization (ISRU) of water ice [2]. Lunar-derived propellants could both decrease the cost of on-orbit refueling and generate revenue, further incentivizing deep space exploration and the development of a cislunar economy [3]. Together, the Vice President's challenge and the Moon's untapped resources offer a unique opportunity: to develop a method for repeatable, crewed lunar surface access that ensures reliability with proven technologies while also preparing for the revolutionary potential of ISRU.

1.2 Scope of the Study

In accordance with the requirements outlined by Theme 3 of RASC-AL 2019, ARTEMIS shall provide transport between Gateway and the lunar surface to allow repeated surface missions near one of the Moon's poles beginning in 2028. The vehicle must accommodate two mission modes: six days on the surface with two crew and 100kg cargo, or two days on the surface with four crew and 500kg cargo. ARTEMIS shall not depend on pre-deployed surface infrastructure but should be capable of evolving beyond its initial capabilities and ultimately leveraging lunar-derived propellants.

This study first presents the overall ARTEMIS mission architecture, subsystem requirements, and specifications. The document then outlines design, development, and testing processes as well as a proposed business strategy, before closing with the architecture's extended capabilities and a risk assessment. Throughout the document, trade studies supported by sensitivity analysis and software simulations are performed to justify design choices with respect to both time and cost.

1.3 Design Summary

The final design for ARTEMIS employs an evolvable 2.5-stage architecture consisting of a crewed lander, uncrewed orbiter, and drop tanks. While the lander and orbiter are reusable from the start of the campaign, drop tanks are initially left on the lunar surface and are repurposed as part of a growing lunar infrastructure. Drop tanks are then matured to full reusability through the anticipated development of lunar ISRU, at which point the vehicle may refuel on the lunar surface and even deliver propellant to lunar orbit. ARTEMIS leverages heritage technologies throughout its design to mitigate risk and cost for early missions, and simultaneously integrates new technologies to provide for an evolvable mission profile.

2 Concept of Operations

2.1 Mission Profile

ARTEMIS begins independent operations once undocked from Gateway in a southern L_2 Near Rectilinear Halo Orbit (NRHO) [4]. The first series of maneuvers, all performed by the orbiter, transfer the vehicle from this initial NRHO to a lunar staging orbit in preparation for landing. These three maneuvers are denoted as Transfer Orbit Insertion (TOI), Low Lunar Orbit Insertion (LLOI), and a Plane Change. TOI occurs at NRHO perilune, placing ARTEMIS on a 110 x 4500km orbit that approaches the Moon over 2.25 hours. The LLOI burn then circularizes the trajectory to a retrograde, 110 x 110km staging orbit with a 92° inclination. Finally, the Plane Change maneuver enables up to 4° of inclination change, giving ARTEMIS the flexibility to reach a variety of identified landing sites between 84°S and 89°S latitude [5]. Figure 1 provides a diagram of this three-burn transfer, including delta-v values calculated from GMAT simulations.

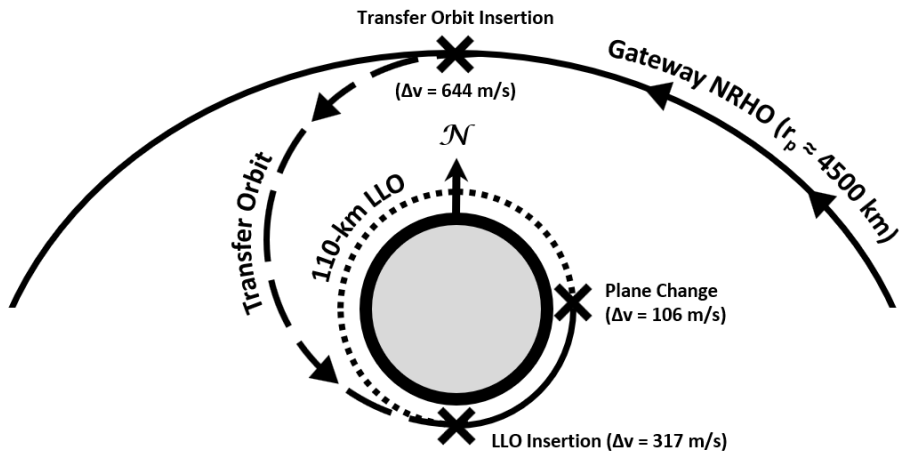

Figure 1: Mission Profile (Gateway to Lunar Staging Orbit)

Following system checkouts in LLO, the crewed lander and affixed drop tanks detach from the orbiter and descend to the lunar surface. The drop tanks serve as the propellant source for all descent and landing burns, which are allocated a delta-v budget of 2012m/s including reserves for hovering. Options for a suitable landing site are numerous, though the Amundsen crater at 84.5°S is a particularly promising candidate due to its diverse lunar geology and the probable presence of water ice [5]. In any case, a site near the South Pole is preferable, as this guarantees line-of-sight for continuous communications with Gateway.

After six days of surface operations, the now-drained drop tanks are removed by the crew prior to launch, and the lander alone performs the 1829-m/s ascent burn back to LLO. The now-drained lander then docks with the orbiter in LLO, and the three-burn transfer in Figure 1 repeats in reverse for return to Gateway. Delta-v requirements for ascent/descent, in addition to the 110km altitude chosen for the staging orbit, are based on the Apollo program [6] [7]. ARTEMIS sizing applies all delta-v values discussed herein and tabulated in Table 2 of Appendix A, with an additional 5% margin for contingency.

2.2 Staging Method

Selection of the 2.5-stage design for ARTEMIS was based on a trade study of four architectures: 2.5 stages (lander, orbiter, and drop tanks), 2 stages (no drop tanks), 1.5 stages (no orbiter), and 1 stage (lander only). The trade study sized each architecture using the previously described delta-v budget and a payload mass of 5.787t. This mass corresponds to the lander's habitable section, common to all staging methods, and includes a 20% margin [8]. Structural coefficients for a lander, orbiter, and drop tanks were based on the Apollo LM descent stage [9] [10], S-IVB [11] [12], and Shuttle External Tank [13], respectively. Given that the former two coefficients are likely conservative estimates, considering advancements since Apollo, the trade study also considered the effect of using lower structural coefficients for an orbiter and lander. Finally, cost estimates were computed via the Rapid Cost Estimation for Space Exploration Systems [14].

Outputs from the trade study, presented as surface plots in Appendix A, motivated the selection of a 2.5-stage design for ARTEMIS. Figure 9 and Figure 10 show the total mass and cost, respectively, of each architecture as a function of varying structural coefficients for an orbiter and lander. For the edge case of highest mass and cost, where the design assumes conservative structural coefficients based on Apollo, the 2.5-stage method outperforms its closest competitors by 14t and $800 million. Assuming modern improvements to the Apollo-era values (i.e. lower structural coefficients), the 2.5-stage method bests all other architectures in terms of mass and all but the 2-stage method in terms of cost. The 2-stage method demonstrates a $500 million cost savings if the lander's structural coefficient can be lowered by 30%, though it notably lacks the extended capabilities of drop tanks for lunar ISRU and on-orbit propellant depots. Given the emphasis placed on extended capabilities for this mission, as well as the relatively minor and non-guaranteed cost savings of the 2-stage method, the 2.5-stage method was selected for ARTEMIS.

2.3 Mission Modes and Surface Operations

The first mission mode, six days on the surface with two crew and 500kg of cargo, is satisfied by following the mission profile to the lunar surface. The crew then completes their surface extravehicular activity (EVA) operations, separate the drop tanks, and return to Gateway. Surface operations for this mission mode are restricted to the EVAs laid out by NASA. The second mission mode, two days on the surface with four crew and 100kg of cargo, requires an extended surface stay. This is due to the Gateway orbital period of 6.5 days; to wait for an optimal rendezvous opportunity with Gateway, the crew spends an extra four days on the surface. Extended surface operations consist of commercial and educational experiments, deployed on the lunar surface to accomplish scientific goals and reduce mission costs for NASA.

3 Structures

3.1 Orbiter

The orbiter is designed to transport the lander between LLO and Gateway. To accomplish this, the orbiter is equipped with a NASA Docking System (NDS) to dock with the lander in LLO. Additionally, the orbiter will undock with the lander when nearing Gateway so that both vehicles may dock separately. This reduces the number of docking ports needed in the ARTEMIS architecture and simplifies the geometry of the lander.

The outer hull of the orbiter is made of intermediate modulus T1100G carbon fiber composite from Toray Advanced Composites. This material was chosen for its extremely high tensile strength (3.46GPa), high elastic modulus (185GPa), and low density (1790kg/m^3) [15]. This combination of properties allows the orbiter to maintain structural integrity while minimizing mass.

The orbiter is also equipped with all propulsion components necessary to carry the lander from the Gateway to LLO and vice versa. This includes fuel tanks, two CECE engines, and helium pressurant. For attitude adjustment and small course corrections, the orbiter is also outfitted with four Reaction Control System (RCS) clusters and RCS fuel. Figure 2 shows the CAD renderings of both the orbiter and lander.

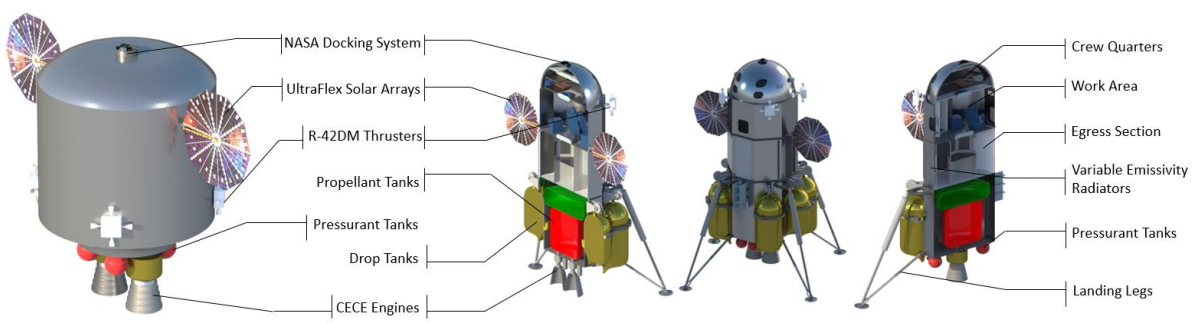

Figure 2: Labeled CAD Renderings of the Orbiter and Lander

3.2 Lander

The lander can be divided into four sections: the crew quarters, work area, egress section, and propulsion section. The crew quarters are located at the top of the lander and is a 1.84m radius pressurized hemisphere with an NDS on top. The work area is a 1.84m radius, 2.13m tall pressurized cylinder. The egress section is a 1.84m radius, 2.4m tall cylinder with a central 1.5m inscribed radius heptagon. The heptagon is pressurized while the area between the cylinder and the heptagon is not. A heptagon shape was chosen so that the Z-2 space suits could easily mount to its surface and allow the astronauts to suit up from inside the lander. The heptagon also has rounded edges to reduce stress concentrations from the internal pressure. Part of the unpressurized area is used for flight avionics, while the bottom 1.25m of the heptagon is used for storing pressurized equipment. Below this, the propulsion section contains fuel tanks, engines, RCS fuel, and helium pressurant. The work area, egress section, and propulsion section are enclosed within a 2m circumscribed radius unpressurized octagon designed for easy mounting of external equipment.

To minimize the weight of ARTEMIS, all structural components are made of the same T1100G carbon fiber composite used on the orbiter. This material was chosen for its extremely high tensile strength (3.46GPa), high elastic modulus (185GPa), and low density (1790kg/m^3). This combination of properties lowers the overall weight of the lander while still preventing ruptures and deformations.

A structural simulation was created to test the performance of the lander's structural components against the pressurized volume and the force of the engines. The resulting maximum displacement is 4mm, and the maximum stress on the body is 514MPa. These results verify that the structure undergoes minimal deformations and the likelihood of stress ever exceeding the composite's tensile strength is extremely low.

The lander is outfitted with landing legs that were designed to ensure safety and reusability. ARTEMIS utilizes four landing legs to maintain symmetry with the octagonal hull and distribute the landing forces as much as possible. As seen in Figure 3, the main struts connect to the hull above and below the drop tanks, and the legs are thin enough to fit between the drop tanks.

Figure 3: The landing legs mounted between two drop tanks.

When extended, the landing legs allow for 0.25m of clearance between the engines and the ground. The legs are made of high modulus carbon fiber utilizing the MS-1A carbon fiber/epoxy resin compression molding system from Toray Advanced Composites. This material is qualified for space applications [16]. All four landing legs combined have a mass of 555.9 kg. An ANSYS structural simulation was designed to test the landing legs. Figure 4 shows the results of the simulation, which shows that the legs undergo very little bending and stress, and the legs can withstand many more cycles than required for its expected lifetime. The landing legs are therefore both safe and reusable.

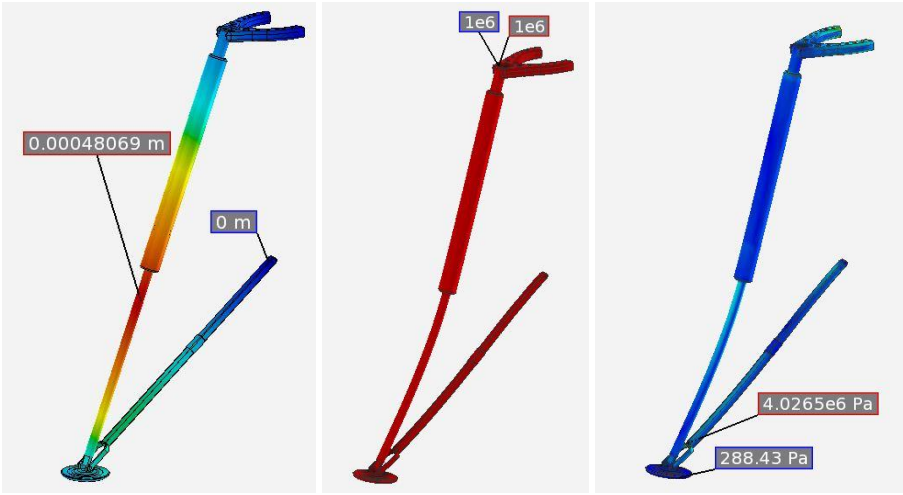

Figure 4: The structural simulation results for the landing legs.

3.3 Drop Tanks

During flight, each drop tank is locked in place by a securing arm and a winch located directly above it. This system prevents all lateral and vertical motion of the drop tanks. The tanks each contain two fuel valves: one near the top for refueling through the lander, and a second valve near the bottom that routes to the engines. This configuration allows the drop tanks to easily refuel and provide fuel, while also mitigating the risk of a valve shearing when the drop tanks are lowered. The fuel interface itself will be based on the Shuttle External Tank [17] as well as contemporary aviation drop tanks.

The entire drop tank lowering process can be performed remotely from inside the lander. To lower the drop tanks, the securing arms are released first, and then the winch is used to slowly lower the drop tank onto the ground. As the drop tank is lowered, it slides down guide rails on the surface of the lander to prevent rotational motions. The bottom of each drop tank is wedge-shaped to ensure that the drop tank tips away from the lander, to avoid damaging the landing legs. On EVA, a crew member then detaches the tanks from the winches and moves them to a more secure location such as a lunar habitat. Importantly, if the drop tanks are not lowered carefully, lunar dust could be kicked up and suspended by electrostatic forces [18]. To mitigate dust contamination, the astronauts will not lower the drop tanks until the end of the surface mission.

4 Vehicle Subsystems

4.1 Power Systems

From Table 6, a maximum power of 4.12kW is required to operate ARTEMIS. To meet this power requirement, UltraFlex solar panels (TRL 9) from Northrop Grumman and 43Ah Space Cells (TRL 9) from EaglePicher Technologies are utilized [19, 20]. The UltraFlex solar panels have powered the Cygnus cargo module and the Phoenix and InSight Mars landers, while EaglePicher batteries have been used on every manned NASA program [21, 22]. UltraFlex solar panels were selected for power generation because of their high power to weight ratio, and 43Ah Space Cells were chosen for their high specific energy. Batteries must also be used to provide power during the LLO phase of the mission when the Moon occults the Sun.

The solar panels are sized to fully recharge the batteries and provide maximum power while the Sun is visible. Therefore, instead of providing 4.4kW of power, the solar panels provide 7.20kW of power. The effects of power generation decay due to radiation are also considered when sizing the solar panels so that they will provide at least 7.20kW. This analysis assumes a power decay rate of 3% per year over 20 years of operation [23]. In order to provide this level of power, each of the two solar panels is 4.33m in diameter.

The 43Ah Space Cells are lithiated nickel cobalt aluminum oxide batteries, and they were selected based on the results of a trade study comparing batteries and fuel cells. While a fuel cell alone would only be 31.08 kg, enough propellant must be brought to operate ARTEMIS for one week in LLO, if the rendezvous with Gateway is missed. With this considered, a power system using fuel cells would need to be 236.67kg, so batteries are the better option. To mitigate the risk of battery failure, the total power load is divided amongst multiple smaller batteries so that one battery failure does not prevent critical systems from getting power. Each Space Cell is 1.27kg, so a total of 66 batteries are needed to operate ARTEMIS.

4.2 Telemetry, Tracking, and Command

Communications systems aboard ARTEMIS consist of a separate system for the lander and the orbiter. The lander will be outfitted with a communication suite derived from the Lunar Laser Communication Demonstration payload flown aboard NASA's LADEE mission [24]. This payload performed successfully in lunar orbit and returned data to the Earth at rates of 622Mbps. This technology was chosen due to its low mass aboard ARTEMIS and record-breaking downlinks and uplinks with the Earth from lunar orbit. The orbiter is outfitted with an S-band communication array to transmit orbiter telemetry and serve as a relay for the lander in case of communication anomalies on the lunar surface. Gateway can also be used as a

communication relay in case of inconsistencies but was chosen as a secondary relay due to the NRHO's period around the Moon.

Command & Data Handling systems for ARTEMIS will consist of a combination of heritage flight controllers and systems that were developed for the Altair lander. This system will consist of three computers voting simultaneously to eliminate points of error. These computers will consist of the heritage quad-core LEON4 microprocessor [25]. Versions of this chipset have already flown to the International Space Station as well as various satellites [26]. This board is already radiation-hardened and will therefore not require additional development to be integrated into ARTEMIS.

4.3 Micrometeorite and Orbital Debris (MMOD) and Radiation Shielding

ARTEMIS uses Whipple shields to mitigate MMOD. ARTEMIS's Whipple shields use aluminum bumper layers with Nextel and Kevlar fabrics as intermediate bumper layers. The former shatters MMOD while the latter disperse them. The Whipple shields will be 198.2kg and cover ARTEMIS's outer hull and crew quarter hemisphere with design variations for different locations. "Stuffed Whipple" shield, a typical design with six layers of Nextel and Kevlar each, is effective against projectiles of up to 1.3cm diameter at 7km/s. Additional shielding can be added after identifying the areas with heaviest MMOD bombardment [27].

While the Kevlar in the MMOD shielding provides some radiation shielding, ARTEMIS utilizes Miralon carbon nanotube sheets (TRL 9) from Nanocomp Technologies, Inc. to supplement the amount of radiation shielding [28]. Miralon was previously used as electromagnetic interference protection on the Juno spacecraft [29]. Carbon was selected because of its very low areal density compared to alternatives such as polyethylene and aluminum. Pure carbon also has a ratio of Atomic Number over Atomic Weight (Z/A) of 0.5, which is comparable to polyethylene's Z/A of 0.571. Additionally, because carbon has a lower atomic number than aluminum, it will produce less neutron backscatter. ARTEMIS will be covered in 20 layers of carbon nanotubes, which is 67.1kg of shielding over the entire lander.

The carbon nanotubes will be attached to the outside of ARTEMIS, and the Whipple shield will be placed on top of the carbon nanotube layer. The orbiter will also be outfitted with carbon nanotubes and a Whipple shield in the same configuration, and the masses of these components are 50.5kg and 151.4kg, respectively.

4.4 Thermal Control

All structural surfaces exposed to space are covered with aluminized mylar to reduce the emissivity of the vehicle to 0.044. Two Variable-Emittance Infrared-Electrochromic Skins (VEIRESs) (TRL 8) from the Ashwin-Ushas Corporation attach to the outer hull and are 1.5m by 2m [30, 31]. The radiators achieve a varying emissivity of 0.19 to 0.72 through a reversible redox reaction. The VEIRESs are also assisted by a 150W heater that can be used when ARTEMIS is under low heat loads. Low heat load is defined as the heat on ARTEMIS when the Moon occults the Sun, and high heat load is defined as the heat on ARTEMIS when exposed to sunlight.

Variable geometry radiators (VGRs) were also considered for ARTEMIS but were deemed too risky due to their low TRL. VGRs change how much heat they reject by altering their geometry. VEIRESs provide a simpler solution over VGRs, and as a result also provide mass, volume, and research time savings as well as less complicated mechanics. The VEIRESs are 9.6kg. An ANSYS thermal simulation was implemented to confirm that the thermal control system can maintain ARTEMIS' temperature effectively. Figure 5 shows that for high heat loads, the thermal control system allows ARTEMIS to maintain a temperature of 18.97℃ to 38.90℃, while for low heat loads, ARTEMIS can maintain a temperature of 18.48℃ to 29.32℃.

50-layer MLI is used on all cryogenic tanks to minimize boil-off of the liquid oxygen (LOX) and liquid hydrogen (LH_2) propellants. All propellant calculations for ARTEMIS also factor in daily boil-off rates, conservatively estimated based on the boil-off rate of the colder LH_2 and factoring in a 7-day margin in

case the Gateway rendezvous is missed. Calculations in Table 4 of Appendix A yielded a boil-off rate of approximately 1% per day, assuming 1.6W/m^2 of heat influx [32].

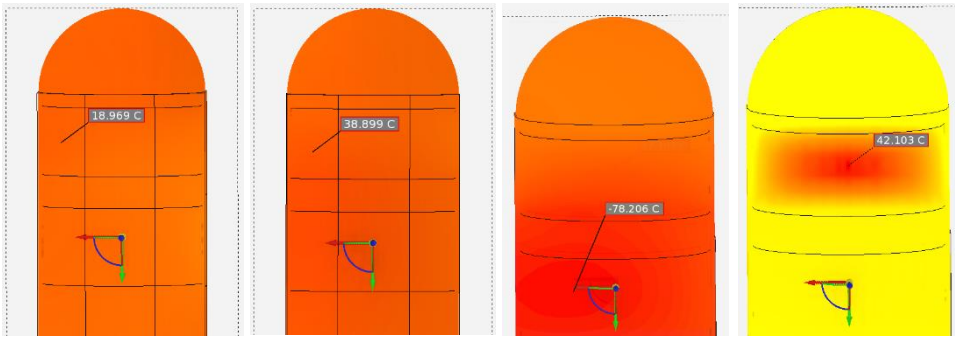

Figure 5: The results of the thermal simulations. The radiators were tested for four cases: high heat load and high emissivity (far left), high heat load and low emissivity (center left), low heat load and high emissivity (center right), and low heat load and low emissivity (far right). For both high and low heat loads, ARTEMIS is capable of maintaining room temperature.

4.5 Propulsion

Four Aerojet Rocketdyne Common Extensible Cryogenic Engines (CECE) (TRL 6) are used on ARTEMIS as the primary propulsion system, with two of these engines on the orbiter and two on the lander [33]. The CECE is a LOX/LH_2 rocket engine with a specific impulse of 445s, tested reliability of 99.95%, and capability of 50 in-space restarts [34]. LOX/LH_2 propellant was selected for its high specific impulse, use in human-rated engines, reduced corrosivity versus hypergolic fuels [35], and potential for in-situ production. Based on the RL10, a highly-successful engine in use for over 50 years [34], the CECE was originally developed as a candidate engine for a crewed lunar lander during the Constellation program [36].

In addition to its flight proven history, the RL10 is already being human rated for CST-100 Starliner [37]. The continued development of the CECE will allow for more restarts as well as improved safety, a trend shown historically by repeated improvements to the Space Shuttle Main Engine over time [38]. Finally, testing of the CECE has also showcased its ability to deep throttle down to 5.9% of rated performance [33], with a specific impulse penalty of 5% [39]. This operational range allows the ARTEMIS lander to both hover at 16% power and ascend with a maximum 6:1 thrust-to-weight ratio. Each CECE can provide 66.7kN of thrust [34], allowing the lander or orbiter to abort with a single engine. This single engine abort is possible as long as the CECE's gimbal range can be increased from its current value of $\pm 4°$ to an enhanced $\pm 10.5°$, in order to point the thrust vector through the center of gravity [40]. This modification is a reasonable area of improvement, as the space shuttle main engine was able to achieve a similar gimbal range [38].

Lunar dust is a notable concern for the CECEs on the lander, as dust has the potential to cause a mechanical failure in the engine [41]. To mitigate this risk, a layer of Mylar is used to cover the portion of the engine ranging from the upper nozzle to the gimbal bearing. Additionally, astronauts will attach a protective cover onto the nozzle during their first EVA on each mission to prevent dust build-up. This cover will be removed from the nozzle prior to ascent to allow it to be reused on future missions.

Propellant masses were used to calculate the sizes of each propellant tank in the orbiter, lander, and drop tanks. Tank dimensions were chosen not only to allow for the proper amount of fuel, but also to allow the tanks to fit inside New Glenn's 7m fairing for delivery to Gateway [42]. In addition to LOX/LH_2, the lander and orbiter each have three externally mounted helium bottles. This helium provides LOX/LH_2 tank pressurization as well as pneumatic pressure for the CECE valves [43].

Refueling of LOX and LH_2 on the lander is done through two ports, co-located on the outside of the main oxygen and hydrogen tanks. When opened, valves allow LOX and LH_2 to also fill all six drop tanks via

these same ports. Each drop tank has its own valve to control fuel inflow. During engine operation on the lander, lines providing fuel from all four LH_2 drop tanks and the main LH_2 tank merge into a common duct that then splits between the fuel pumps of the dual CECEs. Similarly, lines providing oxidizer from the two LOX drop tanks and the main LOX tank merge into a duct that feeds into both CECE oxidizer pumps. All tanks have multiple valves to control where fuel is drawn from during different stages of the mission.

During engine operation on the lander, gaseous hydrogen bled off from both CECEs meets in a common line. This line then splits into five lines that pressurize the LH_2 main tank and drop tanks. Like the ducts providing propellant to the engines, these ducts have valves to control the flow of gaseous hydrogen. Helium on the lander flows from the three helium spheres to all LOX and LH_2 main tanks and drop tanks, as well as the CECEs themselves for pneumatic control, with the helium flow also controlled by valves.

The orbiter's propellant flow systems are similar to those of the lander, with the exception that there are no drop tanks. All orbiter flows are routed to and from the single LOX and LH_2 tanks. Schematics of propellant flow for the lander and orbiter can be seen in Figure 12 and Figure 13, respectively, of Appendix A.

4.6 Reaction Control System

Sixteen Aerojet Rocketdyne R-42DM thrusters are used on both the orbiter and the lander to provide attitude control. The lander and orbiter, combined, require a total 415.2kg of hydrazine and nitrogen tetroxide. This mass was determined by scaling baseline RCS fuel masses from Altair [44]. These propellants, along with LOX, LH_2 and helium are resupplied prior to each mission. In addition to maintaining attitude control throughout descent and ascent, the RCS system provides translation and rotation control during several maneuvers. These maneuvers requiring the RCS system are summarized in Table 11 of Appendix A.

For each mission, the first maneuver involves the lander and orbiter undocking from Gateway. During this maneuver, the lander and orbiter position themselves sufficiently far away from each other and Gateway to ensure that no collision occurs. After undocking from Gateway, the lander and orbiter perform rotations on all axes to verify the health of the RCS systems. This test also positions the lander on a prograde trajectory and the orbiter on a retrograde heading. The undocking maneuver is followed by the docking of the lander and orbiter. When at perilune of the transfer orbit, the RCS system is required to properly orient the lander and orbiter for the burn to circularize into LLO. After undocking from the orbiter in LLO, the lander performs a pitch over maneuver to put itself on a retrograde trajectory for lunar descent.

After lunar ascent, both the lander and orbiter perform standard docking procedures, followed by orienting the lander in the retrograde direction and the orbiter in the prograde direction. At apolune of the transfer orbit, the lander and orbiter orient themselves on a necessary heading to transfer to NRHO. Once near Gateway, the lander and orbiter separate, positioning themselves on a proper orientation for docking.

5 Environmental Control and Life Support Systems (ECLSS)

ARTEMIS contains a $26m^3$ habitable volume. The crew quarter contains a pair of dual navy-standard bunk beds with sleep restraints. A storage area is integrated into the walls above bunks to store consumables, clothing, medical supplies, oxygen masks, and fire extinguishers. Electrochemical windows and LED lighting will be present in each bunk with color cycles to maintain a consistent crew circadian rhythm as part of a Dynamic Lighting Schedule (DLS). Individual crew controls in each bunk enables adjustment of lighting, noise, ventilation, and temperature. The work section contains two permanent seats with storage beneath and two additional retractable seats. Adjacent to these areas are a pair of identical zones. One houses air system hardware, food preparation systems, and medical systems. The other houses waste subsystems. A closable and noise mitigating toilet area provides privacy and a categorized odorless waste storage facility for human and material waste. Air systems are located to facilitate maintenance access and reduce pipeline complexity.

5.1 Atmosphere Baselines and Regulations

ARTEMIS is equipped with a variety of sensors and hardware to meet the baselines for certain air parameters. Equipment is chosen for resource regeneration and mass saving purposes. The air system design also focuses heavily on providing a safe and healthy environment for the crew.

Internal pressure is kept at 101kPa and atmospheric oxygen concentration is maintained at 21%. Humidity is maintained at 40% saturation, while temperature is kept at 296K [45]. The CCAA monitors temperature and controls humidity by condensing water vapor [46]. A CAMRAS scrubs carbon dioxide (CO_2) and moisture, with one spare provided. Its moisture removal capability is inhibited by a desiccant wheel under normal circumstances. If the CCAA fails, CAMRAS can be used to extract moisture without collecting it. The lifespan of sorbent materials is estimated to be 3-5 years, after which replacements are required [47].

The Portable Fan Assembly (PFA) driven ventilation system drives air through coolant loops, CCAA, and CAMRAS, while connecting oxygen and nitrogen tanks to the cabin. Within the ducts, Electrodynamic Dust Shield (EDS) scrubs dust particles. Then, thermal-vacuum regenerable charcoal beds remove waste gas such as methane and ammonia. An ambient temperature catalyst canister removes residual carbon monoxide and hydrogen [48]. Ventilation pipelines are located within the walls surrounding the pressurized area. The ducts can be opened at certain points to inspect fans and mitigate clogging. Vents are located near the corners of the walls to avoid waste air pockets. An independent ventilation system is allocated to supply flight suits.

HEPA-Rated Media filters and packed beds of granular material between the work and egress sections will filter out lunar dust and particulate matter [49]. Four Draper differential mobility spectrometry (DMS) and gas chromatography sensors will be used to measure volatile organic compounds and trace vapor [50]. Major Constituent Analyzer (MCA) constantly monitors partial pressure of various gas, regulating the input of oxygen and nitrogen into the cabin [51].

5.2 Waste Management

ARTEMIS is equipped with the Universal Waste Management System (UWMS). The UWMS (TRL-6) is a compact metabolic waste collection system, equipped with a urine pretreat dose pump and pretreat quality sensor. This system provides an overall mass and volume reduction during exploration- offering the same performance of larger systems at just 80% of the volume. A dual fan/rotary separator with a single motor driving two fans is used to capture waste products and manage odor aboard the lander. Liquid and air are thus separated, with the air being returned to the cabin through a charcoal filtering system. Liquid waste aboard ARTEMIS will be treated using a phosphate-based pretreatment, then delivered to a urine processing system aboard Gateway for recycling purposes at the end of the mission. An anticipated benefit to the UWMS is the development of a low mass and volume fecal canister, reducing logistics and increasing package/stowing efficiency. These canisters could also one day be designed to include water recovery from the stored feces [52].

Additional waste such as food packaging, used clothes, cloths, gloves, and more will be compressed and wrapped into small packages. It will be utilized as a small, additional source of radiation protection aboard the lander until it can be converted into a usable product via a Heat Melt Compactor (HMC) aboard the Gateway. The HMC will recover water from the compact material and produce microbially stable and dry tiles to be used as proper radiation shielding [53].

5.3 Consumables and Habitation

Table 7 illustrates the mass breakdown of daily consumables. Table 8 demonstrates the EVA consumption of supplies. Each day 2.5kg of food, including packaging, is consumed per crew member [54]. Each crew member is allocated 2.8kg of water per day inside the lander: 2kg for drinking, 0.3kg for hygiene, and 0.5kg for food rehydration. Crew members' daily consumption of O_2 is 0.84kg. During EVA, consumption per hour increases to 0.075kg of O_2 and 0.58kg of water; 0.24kg of potable water and 0.34kg for thermal control

[55]. Lander consumables are doubled for redundancy to sustain crew until the next Gateway transfer window.

Food aboard ARTEMIS is rehydrated via a Potable Water Dispenser (PWD). Air supplies are housed in 5000psi pressure vessels. Table 9 shows the tankage space which oxygen and nitrogen occupy. Potable water is housed in twelve 22-liter Contingency Water Containers-Iodine (CWC-I) where iodine and silver ion residual biocide are used as a disinfectant [56]. Condensed vapor and used hygiene water will be contained in separate CWC-I containers.

Four sets of portable breathing apparatus's (PBA) are also supplied. In cases of emergency this self-contained breathing apparatus can sustain a crew member with up to 15 minutes of breathable air, during which repairs can be conducted. In the case of a fire, US orbital segment (USOS) Portable Fire Extinguishers (PFE), which utilize CO_2 as a fire suppressant, are provided. Photoelectric smoke alarms are located inside ventilation system to detect fire [57]. The CCAA's smoke detector serves similar purpose.

5.4 Crew Radiation Mitigation

To provide an accurate characterization of the radiation environment aboard ARTEMIS will contain a combination of active and passive dosimeters. Each crew member will be supplied with a European Crew Personal Active Dosimeter (EuCPAD) that will be worn at all times throughout intravehicular and extravehicular operations. An externally mounted free space PADLES dosimeter and internal Hybrid Electronic Radiation Assessors (HERA) will provide continuous a telemetered data stream and link to the onboard caution and warning systems. Data will be relayed in real-time to ground control and crew.

Each crew member will wear an AstroRad Radiation Vest. The protective material composing these vests have a high density of hydrogen atoms which reduce radiation exposure. These vests will be tested on NASA's uncrewed Orion Exploration Mission 1 (EM-1). The sleeping bag design also contributes to reduced radiation exposure.

5.5 Acoustic Analysis

To fully address the necessary noise mitigation requirements aboard ARTEMIS, the lander will implement a plan to mitigate intermittent and continuous airborne, structural, and enclosure transmitted noise. Airborne sounds are those produced directly from the exposed equipment. This includes the inlets and exhausts of air ducts, or sound which escapes through gaps. This is reduced through investigation of all ducts, ensuring the use of mufflers, resonators, and silencers. Additionally, sound absorbent materials will line the interior and seal the gaps of these noisy ducts. Structure borne noise is defined by the vibrations and subsequent energy transfers from surfaces. It is addressed by using vibration isolators and other damping materials. Enclosure radiated sound is transmitted through the types of closeout materials, such as panels and shelves. Research into the material used to construct these surfaces serves as the main method of mitigation. Damping, viscoelastic materials, and general absorbent material will be utilized to absorb acoustic energy in problematic areas.

Specifically, inlet and outlet mufflers will reduce fan noise whilst other major equipment will be vibrationally isolated using rubber isolators. Duct wrapping and lining, honeycomb closeout panels, viscoelastic coverings, multi-layer blankets and foam barriers will also assist in noise reduction. Ducting lengths and angles will be minimized to prevent additional noise. Crew quarters will act as an isolated enclosure with the connected hatch acting as an additional sound barrier. Flight avionics will be stored in the EGRESS section.

5.6 Spacesuits

The crew will wear Modified Advanced Crew Escape Suits (MACES) brought from the Orion in orbit and during transitions. Z-2 suits with suit ports are chosen for EVAs to mitigate lunar dust hazards. The suit and Portable Life Support System (PLSS) backpack are estimated to be 65kg and 38kg respectively [58]. PLSS' newly developed Rapid Cycle Amine (RCA)(TRL-6), using a concept similar to that of CAMRAS,

removes CO_2 and moisture during EVA. Figure 11 details the interfacing of the Z-2 suit with the suit port [59]. To transfer samples and tools between pressurized and unpressurized areas, a cavity with access to both sides could be developed on the inner hatch. For the same purpose, a container can be integrated onto PLSS. Spacewalks will be conducted by crew wearing their customized Z-2s to transport the suits from the Orion/Gateway to the lander. The Z-2 suits are designed to cope for both in-space and surface usage [60].

6 Gateway Operations

6.1 Resupply and Refueling

The resupply and refueling schedule for ARTEMIS will begin in 2027 starting with the validation mission. An expendable Falcon Heavy will deliver fuel to Gateway every year until the end of ARTEMIS' operational lifetime in 2043. This operational end was chosen due to Gateway's planned operational end in 2043 but can be extended in accordance with any Gateway operational extensions. Starting in 2028 for the first fully crewed mission, resupplies will be delivered to Gateway for ARTEMIS. 1.98t of supplies including empty drop tanks and 7.02t of fuel will be delivered in the 9t co-manifest on the annual SLS-Orion crew launch. These supplies will be used during the lunar mission and remaining supplies will be stored for the following mission. This resupply and refueling schedule will enable all ARTEMIS crewed missions from 2028 to 2043.

Each resupply brings new drop tanks for ARTEMIS to use in its next mission. ARTEMIS takes advantage of Gateway's Next-Generation Canadarm (NGC). When the resupply vehicle arrives at Gateway, the NGC will grab the drop tanks and install them on the lander one at a time. ARTEMIS is outfitted with three NGC attachment points located on the outer hull such that the NGC can maneuver from Gateway and reach each drop tank's final location. Figure 6 shows the locations of the three anchor points on ARTEMIS.

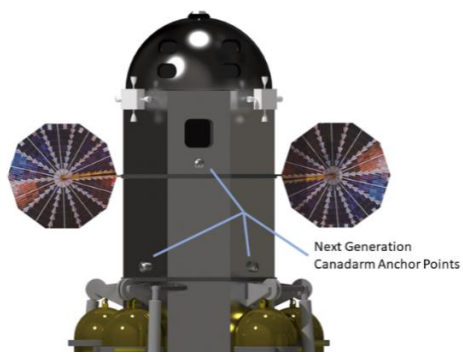

Figure 6: The NGC anchor point configuration on ARTEMIS.

6.2 Gateway Effects

ARTEMIS' primary effect on Gateway is its usage of two NDS modules. The lander and the orbiter will each take up one NDS starting in 2026 through 2043, except for the period where lunar surface missions will occur. Gateway's mass distribution will also be affected when ARTEMIS is fully fueled. This would lead to varying moments of inertia throughout the year for Gateway. This would also affect the station-keeping burns for Gateway in NRHO when ARTEMIS is fully fueled. Although for a short period of time every year, the new mass and moments of inertia would lead to different delta-v numbers required to retain Gateway's southern L_2 NRHO. Another effect that ARTEMIS will have on gateway is the reduced thermal load when the lander or the orbiter is between the Sun and Gateway. ARTEMIS' thermal control system would dissipate this energy, relieving Gateway of the extra load.

6.3 Uncrewed Operations

During the 11-month period when neither ARTEMIS nor Gateway is crewed, ARTEMIS will function in a dormant state in which regular checks will be performed to demonstrate continued flight capability.

Biweekly tests on the ECLSS systems will ensure that the system remains up to date and the smallest of inconsistencies are detected and mitigated immediately. The valves and equipment in the propellant flow systems will undergo monthly tests to ensure optimal functionality. The solar panel actuators and VEIRESs will be tested monthly to confirm nominal operation of the power system and thermal control system on board ARTEMIS. In case of anomalies in any tests, the resupply manifest for the following mission will be modified to include parts and updates necessary to mitigate and correct the off-nominal processes.

7 Design, Development, and Testing

7.1 Design and Development

The first phase of design and development for ARTEMIS is already underway, culminating in the system-wide concept study detailed in this report. Following an independent review of the concept study herein, the system will be ready to proceed into technology development and preliminary design by late 2019. The heritage structural and propulsive elements of the architecture is developed in conjunction with the Z-2 spacesuits and the drop tank system. These revolutionary technologies have been a part of previous NASA studies and are developed to fruition for ARTEMIS [61] [62]. This design phase lasts for two years, as shown in Figure 7, and ends with the finalization of all design requirements and specifications. Design requirements for a static model of the lander are also outlined in this time to begin crew training by 2022.

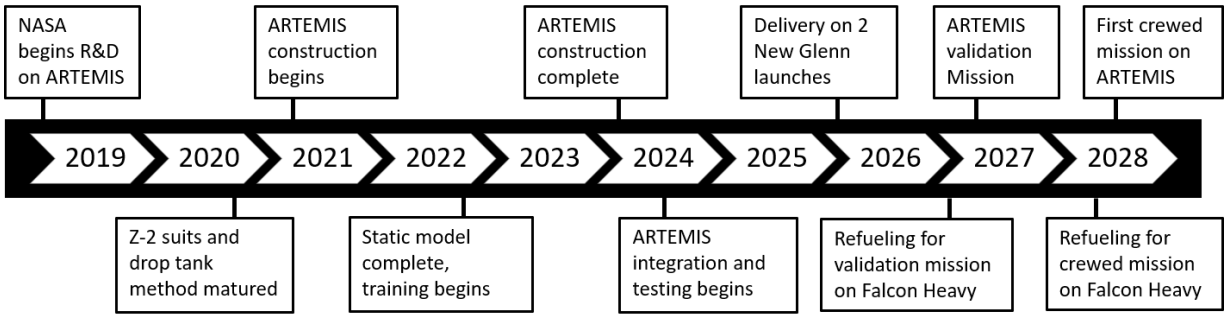

Figure 7: ARTEMIS Development Timeline

7.2 Procurement, Manufacturing, and Testing

The procurement plan for ARTEMIS consists of two phases of Invitations to Tenders (ITTs). The first ITT phase invites NASA prime contractors to manufacture major ARTEMIS systems. The structural, propulsive and ECLSS systems for the lander and the orbiter are contracted in a manner similar to Maxar Technologies' contract for Gateway's Power and Propulsion Element [63]. The second phase of ITTs are used by the recipients of the first ITT. Subsystem contracts are assigned for manufacturing as per the design requirements set by NASA. Starting in 2021, construction begins at NASA's Michoud Assembly Facility. This facility was chosen due to its capability to enable all construction at one site and its proximity to a port [64]. The static model of the lander is delivered to Johnson Space Center in 2022 to begin astronaut training.

ARTEMIS integration and testing begins in 2024 at NASA's Plum Brook Facility in Ohio. The lander and orbiter flight articles are first tested individually for a series of acceptance tests. They are then mated together and tested in the Reverberant Acoustic Test Facility and the Mechanical Vibration Facility. These tests subject ARTEMIS to the acoustic and vibration profiles that the lander and orbiter experience on launch. The CECE engine is simultaneously tested at Plum Brook's In-Space Propulsion Facility to prove its restart capability using an updated version of the testing regime from 2009 [36]. ARTEMIS is then moved into Space Simulation Vacuum Chamber to perform environmental duty cycle testing. This phase of the testing for ARTEMIS lasts for an extended period due to its high operational lifetime of 15 years.

7.3 Launch and Validation

When all testing is complete, ARTEMIS is transported to Cape Canaveral Air Force Station (CCAFS) for final checkout and pre-launch operations. Two New Glenn rockets are launched from Blue Origin's LC-

36, one each for the lander and the orbiter. This launch system was chosen because of its 7m payload fairing which allows for an increased payload volume. The landing legs are folded to fit inside the fairing and the lander is outfitted with the drop tanks for the initial launch. Both the lander and the orbiter are launched dry and then fueled by an expendable Falcon Heavy launched from LC-39A at CCAFS in 2027. The expendable variant of the Falcon Heavy was chosen for its capability to deliver 20.3t of fuel to Gateway's orbit. This 2027 refueling mission is used to supply for the validation mission set to occur the same year. This mission manifest includes a two-pilot crew that undocks from Gateway and reach the lunar surface by following the predefined mission profile. The drop tanks are then separated on the surface and an ascent burn is performed to reach LLO. The lander then docks with the orbiter and arrives at Gateway to demonstrate the capability to carry crew and cargo to the lunar surface. Annual crewed missions starting in 2028 follow until the end of the architecture's operational lifetime in 2043, consistent with Gateway's planned operational timeframe.

8 Business Plan

A cost breakdown as well as a business plan was generated for ARTEMIS using NASA's Project Cost Estimating Capability. A project cost breakdown for ARTEMIS is shown in Figure 8. Surface costs for ARTEMIS before launch from 2019-2026 require US$ 5.7 billion. These costs include the design, development, manufacturing, integration, and testing for the architecture. Launch and the validation mission in 2026 and 2027 respectively bring the cost up to US$ 5.9 billion. Annual crewed missions from 2028-2043 bring the total ARTEMIS mission cost to US$ 8.25 billion.

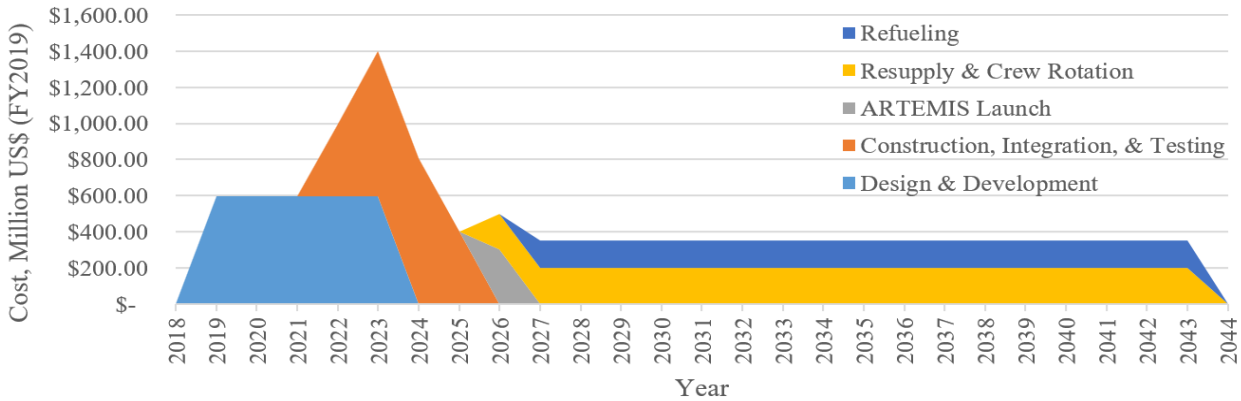

Figure 8: ARTEMIS Cost Breakdown by Category

A business plan for ARTEMIS consisting of international and commercial partnerships is proposed. Components of ARTEMIS can be contracted to international space agencies such as ESA as was done with the Orion MPCV's service module [65]. A contract with international agencies to bring astronauts aboard ARTEMIS will benefit both parties. Contracts with commercial partners to deliver payloads to the lunar surface are considered for the extended lunar surface stay for missions following the second mission mode. The extra time on the lunar surface will be used to carry out experiments for these partners. A mission cost split consisting of 60% of the contributions coming from NASA and 20% each coming from international and commercial partners enables new countries and corporations to access the lunar surface and save NASA US$ 3.3 billion, bringing total mission cost for NASA down to US$ 4.95 billion.

9 Extended Capabilities

ARTEMIS is designed to support and integrate with an evolving lunar surface infrastructure. Each element of ARTEMIS can evolve or be repurposed independently, while the collection of all elements can mature to full reusability with the development of lunar ISRU.

Early ARTEMIS missions leverage disposable architecture elements to accelerate the development of lunar surface infrastructure. Drop tanks left on the surface of the Moon may be repurposed for MMOD or

radiation shielding, resource storage, or habitat construction. Vehicles from refueling missions can be repurposed as propellant depots either in cis-lunar space or at Gateway.

Later ARTEMIS missions leverage the establishment of lunar ISRU to achieve full reusability. Using lunar regolith derived LH2/LOX propellant, drop tanks from prior missions can be refueled and attached to landers from subsequent missions to assist in ascent. This allows ARTEMIS to deliver 5.4t of propellant from the Moon back to LLO, which in turn facilitates further development of the previously mentioned cis-lunar propellant depots. Residual propellant from missions may be stored upon return to Gateway, which may be further leveraged with the development of zero boil-off technology.

10 Risk Assessment Matrix

Table 1: Pre-Mitigation (Left) and Post-Mitigation (Right) Risk Matrix

		Consequence								Consequence				
		1	2	3	4	5				1	2	3	4	5
Likelihood	5							Likelihood	5					
	4			3					4					
	3		5						3					
	2				1 12	10 11			2		1 12	3	11	
	1					2 4 6 7 8 9			1	8	4 5	2 6 7 9 10		

1	Failure to raise drop tank TRL	7	Fuel tank rupture
2	Landing leg buckling	8	Battery failure
3	Cannot land/abort near surface	9	Solar panel failure
4	Missed Gateway transfer window	10	Air system breakdown
5	Communication system failure	11	Oxygen/Hydrogen/Helium tank rupture
6	Propulsion system failure	12	Failure to raise Z-2 suit TRL

Table 1 identifies risks within the ARTEMIS architecture and illustrates how mitigation strategies both reduce the likelihood and impact of those risks.

Landing legs buckling on the surface of the Moon will cause the vehicle to tip over, resulting in catastrophic failure. This is mitigated by an immediate abort to LLO. Drop tanks on ARTEMIS are designed to release along guide rails, which allows them to be detached safely even in-flight, making an abort to orbit feasible.

If the lander is unable to land on the lunar surface, a near-surface abort would be initiated. Without jettisoning the drop tanks, the lander would require a larger amount of delta-V to reach LLO. This allows for less time for the abort to be initiated than if the drop tanks were detached. Releasing the drop tanks in flight using the winch and guide rails decreases the delta-V required to reach LLO, allowing an abort closer to the ground. Not only does this allow more time for a decision to be made, but it also gives more room for error in the event that the vehicle is not functioning at peak performance.

If a transfer window to Gateway is missed, the crew must remain in LLO for seven days before the next window. To accommodate for this possibility, life support, fuel, and power systems are selected and sized to accommodate for 14 days of consumption/usage, such that a backup opportunity may be pursued.

While loss of communications does not directly result in mission failure, it inhibits connectivity between the crew and ground control, potentially delaying the transmission of critical information. This is mitigated by having both the orbiter and Gateway serve as redundancies to relay communication back to Earth.

Propulsion system failure results in loss of mission with the crew stranded in deep space. Both the lander and orbiter are designed with two CECE engines such that the crew can safely abort the mission if one engine fails. The remaining engine aligns its thrust vector with the vehicle's center of mass. If the TRL of the CECE is not raised to provide enough gimbal range, RCS will be used to supplement engine gimbal.

Fuel tank rupture due to MMOD impact could result in mission failure, but the 2.5-stage architecture allows ARTEMIS to retain partial functionality in such events. If one of three fuel systems — drop tanks, lander, or orbiter — remains intact, the crew can always abort when in LLO or a higher orbit. When on the lunar surface, damage to the lander fuel tanks can be mitigated by transferring fuel to the drop tanks.

If the batteries were to fail during the mission, the crew would not have any life support when the solar panels cannot provide power. This would result in a catastrophic failure. To mitigate this, the power load is distributed amongst 66 batteries so if one battery fails, life support systems can still get power. Additionally, EaglePicher batteries were selected in part for their superior reliability. Over more than two billion cell hours in space, an EaglePicher battery has never caused a single failure [21].

A total loss of power from the solar panels would result in catastrophic failure because the lander only has enough batteries to last for approximately 85 minutes of peak power usage. Crew could lengthen their survival time by shutting off nonessential systems, but it is nearly impossible to make that power supply last until the Gateway returns. In order to mitigate this risk, the power supply is split between two Ultraflex solar panels. One solar panel can produce enough power to keep all essential systems operational, even at the end of the solar panel's lifespan. Additionally, the UltraFlex solar panels have been used extensively for the Cygnus cargo module, as well as the Phoenix and InSight Mars Landers [22]. It is unlikely that a system with this much previous use would abruptly and totally fail.

If ventilation system experiences fan failures or clogging, accesses located on the pipelines allow the crew to mitigate the problem. Screens within ventilation removes large particles, preventing clogging problems. CAMRAS' reduced size and weight allow one spare to be brought onboard for substitute. If CCAA fails, CAMRAS can remove vapor without collection. However, CCAA failure still requires immediate actions to restore its temperature control capability. Flight suits and oxygen masks can protect the crew during such transition period and repairment sessions. The isolated ventilation system for flight suits can also serve as backup when the primary one fails.

If an oxygen or hydrogen tank were to rupture, fundamental life support systems would be unavailable to the crew. This means that the crew would be unable to regulate the atmosphere or provide an air supply for flight suits. This can be catastrophic, so immediate repairs are necessary. Spare CAMRAS for CO2 and moisture removal can be utilized, in addition to supplied oxygen masks.

Design and development risks are mainly caused by delayed or failed TRL maturity. If the TRL of drop tank technology cannot be raised sufficiently in the proposed development timeline, ARTEMIS cannot meet the 2028 mission requirement, and may risk significant cost increases or even cancellation. To mitigate this risk, ARTEMIS can descope by fixing the drop tanks permanently to the lander. This design change would effectively create a 2-stage architecture, eliminating the TRL risk of drop tanks at the expense of scaling up the entire system and losing most extended capabilities.

Insufficient TRL maturity of Z-2 suits results in the need for customized suits for each astronaut delivered to Gateway before lunar missions. Custom Z-2 suits also require extra EVA procedures to be performed at Gateway to replace old suits with new ones. Mass is allocated in resupply missions to account for extra shipments of the Z-2 suits, such that the extra resupply demand will not exceed launch vehicle limitations.

Appendix A: Calculations and Tables

Table 2: Delta-v Budget*

Mission Phase	Maneuver	Initial Position	Final Position	Stage	Delta-v (m/s)
Inbound to Moon	Transfer Orbit Insertion	L_2 South NRHO	110 x 4500km Transfer Orbit	Orbiter	644
	LLO Insertion	110 x 4500km Transfer Orbit	110km LLO (92° inclination)	Orbiter	317
	Plane Change	110km LLO (92° inclination)	110km LLO (84° inclination)	Orbiter	106
	Descent & Landing	110km LLO (84° inclination)	Lunar Surface	Drop Tanks	2012
Outbound from Moon	Ascent	Lunar Surface	110km LLO (84° inclination)	Lander	1829
	Plane Change	110km LLO (84° inclination)	110km LLO (92° inclination)	Orbiter	106
	Transfer Orbit Insertion	110km LLO (92° inclination)	110 x 4500km Transfer Orbit	Orbiter	317
	NRHO Insertion	110 x 4500km Transfer Orbit	L_2 South NRHO	Orbiter	644
				Total	5975
				Total + 5% Contingency Margin	6274

* Does not include delta-v for attitude control

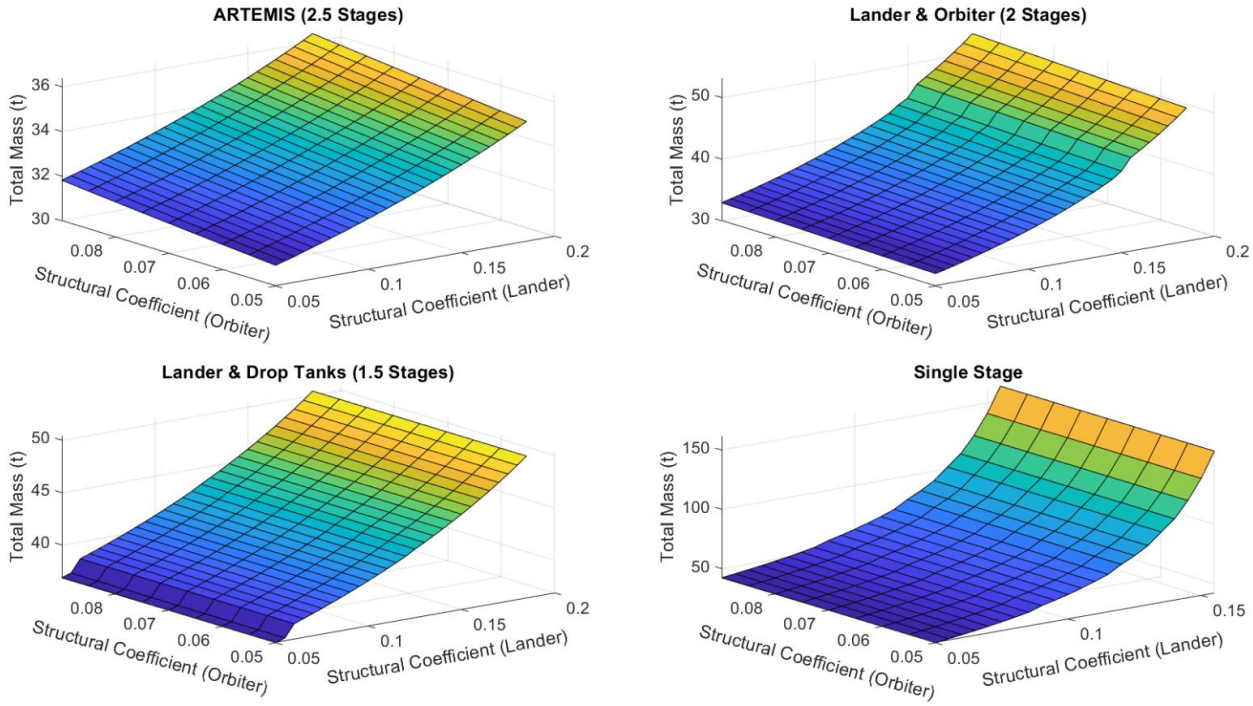

Figure 9: Staging Trade Study: Total Mass with Varying Structural Coefficients (Note: Reduced X-Y Scale for Single Stage, for Ease of Comparison)

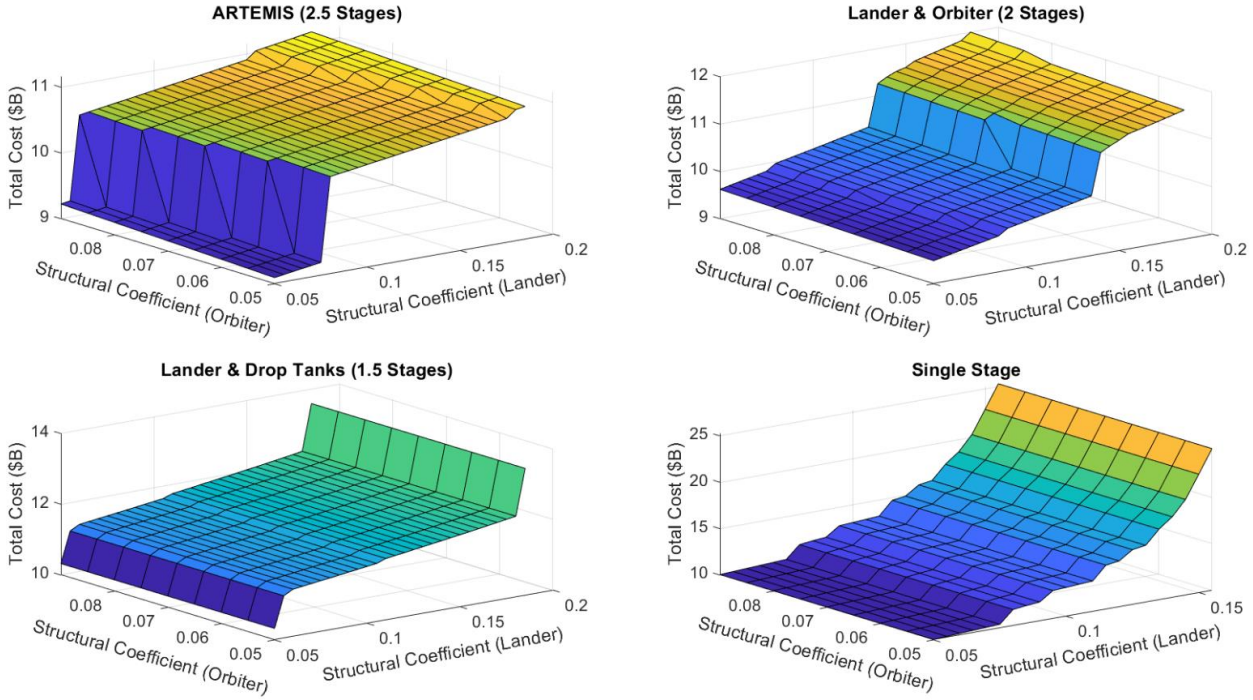

Figure 10: Staging Trade Study: Total Cost with Varying Structural Coefficients (Note: Reduced X-Y Scale for Single Stage, for Ease of Comparison)

Table 3: Mass Budget

Vehicle Section	Vehicle Subsection	Subsystem	Mass (t)
Lander	*Habitable Section*	ECLSS	2.193
		ADCS	0.280
		GN&C	0.090
		C&DH	0.131
		Communications	0.030
		Power	0.171
		Thermal Control	0.010
		Structures	1.439
		MMOD/Radiation Shielding	0.155
		NDS Docking Port	0.324
		Subtotal	**4.823**
		Subtotal + 20% Margin	**5.787**
	Propulsion Section	2 Engines (CECE)	0.318
		Landing Legs	0.555
		MMOD/Radiation Shielding	0.110
		Remaining Structure	0.667
		Propellant (LOX/LH_2)	5.382
		Subtotal	**7.032**
Drop Tanks		Structure	0.455
		Propellant (LOX/LH_2)	9.228
		Subtotal	**9.683**
Orbiter		2 Engines (CECE)	0.318
		Power	0.009
		Communications	0.022
		MMOD/Radiation Shielding	0.202
		NDS Docking Port	0.324
		Remaining Structure	1.154
		Propellant (LOX/LH_2)	11.809
		Subtotal	**13.836**
Totals		**Dry Mass**	9.920
		Propellant Mass	26.419
		Wet Mass	36.338

Table 4: Liquid Hydrogen Boil-off Calculations

Constants	Heat Flux into Tank (w/ 100% Margin) [32]	1.6 W/m^2
	Heat vs. Boil-off Relation [32]	0.2 kg/day/W
Tank Surface Area	Lander Tank	26.95 m^2
	Single Drop Tank	14.55 m^2
	Orbiter Tank	45.57 m^2
Heat Influx	Lander Tank	43.12 W
	Single Drop Tank	23.28 W
	Orbiter Tank	72.91 W
Boil-off Rate	Lander Tank	8.62 kg/day
	Single Drop Tank	4.66 kg/day
	Orbiter Tank	14.58 kg/day
Boil-off Rate (% of Total)	Lander	1.17 %/day
	Single Drop Tank	1.37 %/day
	Orbiter	1.02 %/day

Table 5: ECLSS Mass Budget

Subsystem	2-Crew Missions (kg)	4-Crew Missions (kg)
Water	133.84	267.68
Food	70	140
Oxygen	34.54	61.90
Nitrogen	23.62	23.62
EVA Suits	206	412
Crew Members*	160.06	320.13
Flight Suits	83.4	166.8
AstroRad Vests	10	20
Hygiene	39.2	78.4
Cargo	500	100
Food Containers	51.32	102.65
Oxygen Vessels	12.57	22.53
Nitrogen Vessels	40.16	40.16
Air System	226.14	226.14
Medical System	136	136
UWMS	75	75
TOTAL	**1801.84**	**2193**

* Astronaut weight is estimated using equal number of male and female in both cases.

Table 6: Power Budget

Subsystem	Power Consumption (kW)
Water	0.5
Food	0.6*
Lighting	0.1
Atmosphere Regulation	1.5
Docking	0.25
Sensor Suite	0.2
Star Tracker	0.2
Communication	0.12
UWMS	0.15
Total	**3.62**

*The value is based on short-term peak consumption.

Table 7: Lander Consumables Mass Breakdown [55]

Consumable	Amount consumed (kg/day/Crew Member)
Food (with packaging)	2.5
Drinking Water	2
Hygiene Water	0.3
Food Rehydration Water	0.5
Oxygen	0.84

Table 8: EVA Consumables Mass Breakdown [55]

Consumable	Amount consumed (kg/hour/Crew Member)
Drinking Water	0.24
Thermal Control Water	0.34
Oxygen	0.075

Table 9: Pressure Vessel Volume

	2-Crew Missions (liter)	4-Crew Missions (liter)
Oxygen	77	151
Nitrogen	60	60

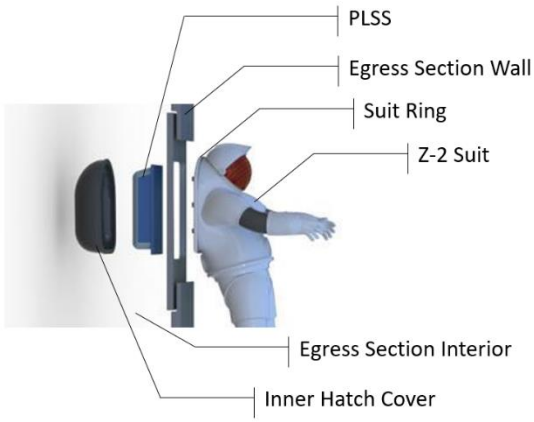

Figure 11: Z-2 Suit Port Interface [60]

Table 10: Pressure Vessel Volume

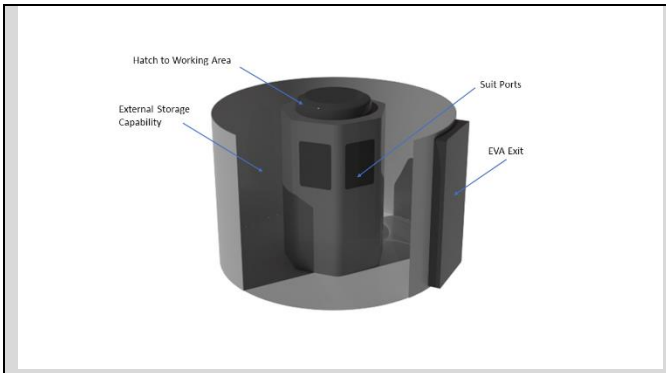	**2-Crew Missions (liter)**	**4-Crew Missions (liter)**
Oxygen	77	151
Nitrogen	60	60

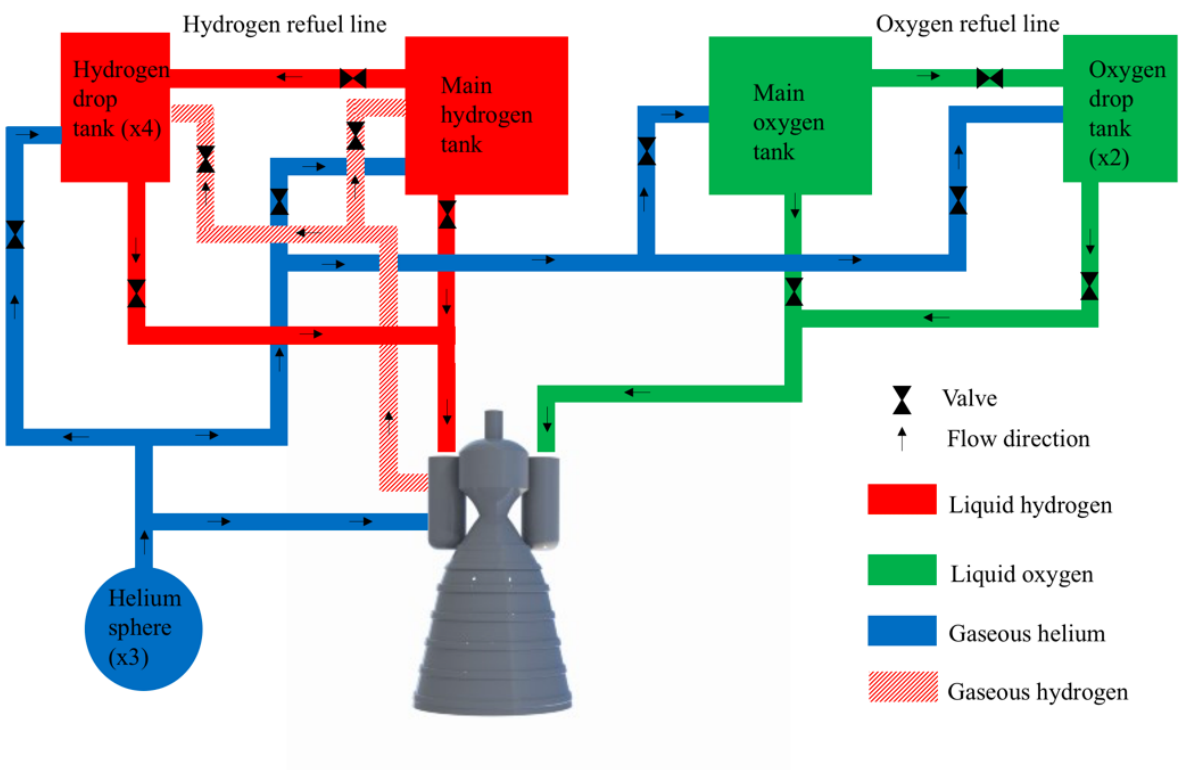

Figure 12: Lander Propellant Flow Schematic

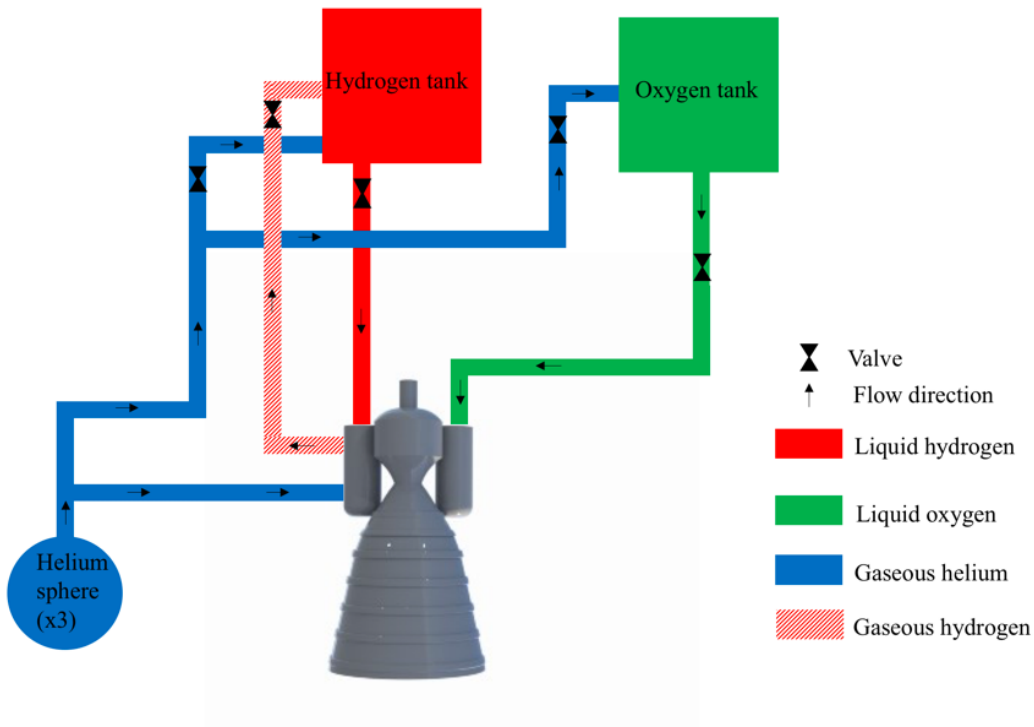

Figure 13: Orbiter Propellant Flow Schematic

Table 11: Maneuvers Requiring Use of RCS

#	Maneuver Description	Location	Orientation
1	Orbiter undocking and RCS test	Gateway	Rotations about roll, yaw, and pitch axis
2	Position orbiter for docking sufficiently far from Gateway	Gateway	Retrograde
3	Lander undocking and RCS test	Gateway	Rotations about roll, yaw, and pitch axis
4	Position lander for docking sufficiently far from Gateway	Gateway	Prograde
5	Lander and orbiter docking	Near Gateway	Prograde (Lander); Retrograde (Orbiter)
6	Reposition to enter LLO	Transfer Orbit	Prograde (Lander); Retrograde (Orbiter)
7	Lander undocking and positioning for descent	LLO	Retrograde
8	Lander attitude control during descent and landing	Lunar Descent	Retrograde; Hover
9	Lander attitude control during ascent	Lunar Ascent	Prograde
10	Lander and orbiter docking; Reposition for transfer orbit burn	LLO	Retrograde (Lander); Prograde (Orbiter)
11	Reposition to transfer to NRHO	Transfer Orbit	Retrograde (Lander); Prograde (Orbiter)
12	Lander and orbiter undocking; Reposition for gateway docking	Near Gateway	In line with Gateway docking ports
13	Lander docking with Gateway	Gateway	In line with Gateway docking ports
14	Orbiter docking with Gateway	Gateway	In line with Gateway docking ports

Appendix B: Theme Compliance Matrix

Table 12: Theme Requirement Compliance Matrix

Requirement	Location
Come up with concepts for crewed lunar surface access and a campaign that allows repeated surface missions to establish a research station at or near one of the Moon's poles.	Page 1, Design Summary
The architecture should leverage current NASA capability investments, as well as existing or anticipated (near-term) commercial and international launch vehicles, in space propulsion capabilities, and lunar surface systems.	Page 7, Propulsion Page 12, Design and Development
Architectures cannot be dependent on lunar-derived in-situ resources at the beginning, …	Page 1, Design Summary
… but should be capable of evolving into an architecture that could leverage some lunar developed propellants if/when they become available.	Page 1, Design Summary
Crew is delivered from Earth to Gateway via NASA's Space Launch System and Orion.	Page 11, Resupply and Refueling
Crew returns to Earth from Gateway via Orion.	Page 11, Resupply and Refueling
A reusable ascent/descent cabin/vehicle is based at Gateway, where it is resupplied and refueled between lunar missions.	Page 1, Mission Profile
Mission mode 1 — 6 days on the surface with 2 crew and 500 kg of cargo – no pre-deployed support infrastructure.	Page 3, Mission Modes and Surface Operations
Mission mode 2 — 2 days on the surface with 4 crew and 100 kg of cargo – longer stays enabled by pre-deployed infrastructure (rovers, habitats, etc.).	Page 3, Mission Modes and Surface Operations
Both above mission modes must also accommodate the crew during their transit to and from the lunar surface.	Page 8, Environmental Control and Life Support Systems (ECLSS)
Initial architecture and program model that is not "dead-ended" and facilitates evolution from initial capability to a model that leverages commercial services in order to reduce costs for sustained crew access to the lunar surface.	Page 13, Business Plan Page 13, Extended Capabilities
Consider impact of elements on the Gateway (controllability, power, thermal, etc.).	Page 11, Gateway Effects
Consider number of SLS launches (ideal would be one per human lunar mission once the reusable ascent/descent vehicle is delivered to the Gateway with the remaining launches provided by commercial or international partners).	Page 11, Resupply and Refueling
Consider technology readiness and cost to support a crewed lunar mission from the Gateway in 2028.	Page 12, Design, Development, and Testing
Proposed designs should be consistent with human spacecraft requirements addressed in NASA Technical Standards 3000 and 3001 and NASA's Human Integration Design Handbook (HIDH), and the physiological countermeasures identified in NASA standards should be addressed.	Page 8, Environmental Control and Life Support Systems (ECLSS)

Appendix C: References

[1] NASA/Goddard Space Flight Center, "Human Landing System - Integrated Lander Pre-Solicitation NNH19ZCQ001K_APP-H," 26 April 2019. [Online]. Available: https://www.fbo.gov/index?s=opportunity&mode=form&tab=core&id=5dcac498e0b7b8def42dea1068b1eab7. [Accessed 21 May 2019].

[2] S. Li, P. G. Lucey, R. E. Milliken, P. O. Hayne, E. Fisher, J.-P. Williams, D. M. Hurley and R. C. Elphic, "Direct Evidence of Surface Exposed Water Ice in the Lunar Polar Regions," *Proceedings of the National Academy of Sciences*, vol. 115, pp. 8907--8912, 4 September 2018.

[3] D. Kornuta, A. Abbud-Madrid, J. Atkinson, J. Barr, G. Barnhard, D. Bienhoff, B. Blair, V. Clark, J. Cyrus, B. DeWitt, C. Dreyer, B. Finger, J. Goff, K. Ho and L. Ke, "Commercial Lunar Propellant Architecture: A Collaborative Study of Lunar Propellant Production," *REACH*, vol. 13, no. 2352-3093, p. 100026, 2019.

[4] J. Williams, D. E. Lee, R. J. Whitley, K. A. Bokelmann, D. C. Davis and C. F. Berry, "Targeting Cislunar Near Rectilinear Halo Orbits for Human Space Exploration," in *27th AAS/AIAA Space Flight Mechanics Meeting*, San Antonio, 2017.

[5] M. Lemelin, D. M. Blair, C. E. Roberts, K. D. Runyon, D. Nowka and D. A. Kring, "High-priority lunar landing sites for in situ and sample return studies," *Planetary and Space Science*, no. 101, pp. 149-161, 2014.

[6] Manned Spacecraft Center, "Apollo 11 Flight Plan," NASA, Houston, 1969.

[7] Manned Spacecraft Center, "Apollo Lunar Landing Mission Symposium," in *Proceedings of the Apollo Lunar Landing Mission Symposium*, Houston, 1966.

[8] J. R. Wertz, D. F. Everett and J. J. Puschell, Space Mission Engineering: The New SMAD, Microcosm Press, 2011.

[9] NASA Space Science Data Coordinated Archive, "Apollo 11 Lunar Module / EASEP," NASA, [Online]. Available: https://nssdc.gsfc.nasa.gov/nmc/spacecraft/display.action?id=1969-059C.

[10] Grumman, "Main Propulsion Quick Reference Data," NASA.

[11] Marshall Space Flight Center, NASA, "Technical Information Summary AS-501 (Apollo Saturn V Flight Vehicle)," NASA, Huntsville, 1967.

[12] Marshall Space Flight Center, NASA, "J-2 Engine Fact Sheet," NASA, Huntsville, 1968.

[13] Caltech/JPL, "Ask an Astronomer: How Much Did the Space Shuttle Weigh?," California Institute of Technology, [Online]. Available: http://coolcosmos.ipac.caltech.edu/ask/268-How-much-did-the-Space-Shuttle-weigh-.

[14] D. C. Arney and A. W. Wilhite, "Rapid Cost Estimation for Space Exploration Systems," in *AIAA SPACE 2012 Conference & Exposition*, Pasadena, 2012.

[15] Toray Composite Materials America, Inc, "Types of Carbon Fiber," [Online]. Available: https://www.toraycma.com/page.php?id=661. [Accessed 29 May 2019].

[16] Toray Advanced Composites, "Product MS-1A," [Online]. Available: https://www.toraytac.com/product-explorer/products/deaZ/MS-1A. [Accessed 29 May 2019].

[17] J. Wilson, "Space Shuttle: The External Tank," NASA, 5 March 2006. [Online].

[18] C. M. Katzan and J. L. Edwards, "Lunar Dust Transport and Potential Interactions With Power System Components," NASA, 1991.

[19] Northrop Grumman, "UltraFlex Solar Array Systems," 2018. [Online]. Available: https://www.northropgrumman.com/Capabilities/SolarArrays/Documents/UltraFlex_Factsheet.pdf. [Accessed 16 January 2019].

[20] EaglePicher Technologies, "43Ah Space Cell," [Online]. Available: https://www.eaglepicher.com/sites/default/files/LP%2033450%2043Ah%20Space%20Cell%20%200319.pdf. [Accessed 29 May 2019].

[21] EaglePicher Technologies, "FAQs," [Online]. Available: https://www.eaglepicher.com/about-us/faqs/. [Accessed 30 May 2019].

[22] J. Rhian, "ATK's Lighter, Stronger Solar Arrays to Power Orion," 24 October 2012. [Online]. Available: https://www.americaspace.com/2012/10/24/atks-lighter-stronger-solar-arrays-to-power-orion/. [Accessed 30 May 2019].

[23] T. Girish and S. Aranya, "Moon's Radiation Environment and Expected Performance of Solar Cells During Future Lunar Missions," arXiv, 2010.

[24] NASA GSFC, "The Lunar Laser Communication," 28 May 2013. [Online]. Available: https://alumni.jhu.edu/sites/default/files/inline-images/NASA-LasercomTalk-JHU-Aerospace-Affinity-June-11th-2014.pdf. [Accessed 26 May 2019].

[25] Aeroflex Gaisler, "Quad-Core LEON4 Next Generation Microprocessor," May 2012. [Online]. Available: http://microelectronics.esa.int/gr740/NGFP-BPROD-0017-i1r0.pdf. [Accessed 27 May 2019].

[26] European Space Agency (ESA), "Leon's First Flights," ESA, 2019. [Online]. Available: http://www.esa.int/Our_Activities/Space_Engineering_Technology/LEON_s_first_flights. [Accessed 27 May 2019].

[27] E. L. Christiansen and D. M. Lear, "Micrometeoroid and Orbital Debris Environment & Hypervelocity Shields," National Aeronautics and Space Administration, 2012, Houston.

[28] Nanocomp Technologies, Inc, "Miralon Sheets/Tape," [Online]. Available: http://www.miralon.com/sheet/tape?hsCtaTracking=3d204392-0669-41cb-8942-1aa33ea75cbe%7Cc2811465-fb95-4fd7-ad96-4f6f206b6aef. [Accessed 29 May 2019].

[29] Nanocomp Technologies, Inc, "Miralon in Aerospace & Defense," [Online]. Available: http://www.miralon.com/aerospace-defense. [Accessed 29 May 2019].

[30] Ashwin-Ushas Corporation, "Variable-Emittance Infrared (IR)-Electrochromic Skins for Spacecraft Thermal Control," [Online]. Available: https://ashwin-ushas.com/developed-technologies/variable-emittance-infrared-ir-electrochromic-skins/#description. [Accessed 29 May 2019].

[31] Ashwin-Ushas Corporation, "FORM B - PROPOSAL SUMMARY," 15 December 2011. [Online]. Available: https://sbir.nasa.gov/SBIR/abstracts/10/sbir/phase2/SBIR-10-2-X3.04-8984.html. [Accessed 29 May 2019].

[32] C. B. Muratov, V. V. Osipov and V. N. Smelyanskiy, "Issues of Long-Term Cryogenic Propellant Storage in Microgravity," NASA NTRS, 2011.

[33] V. J. Giuliano, T. G. Leonard, R. T. Lyda and T. S. Kim, "CECE: Expanding the Envelope of Deep Throttling Technology in Liquid Oxygen/Liquid Hydrogen Rocket Engines for NASA Exploration Missions," NASA NTRS, 2010.

[34] Aerojet Rocketdyne, "Common Extensible Cryogenic Engine," [Online]. Available: https://web.archive.org/web/20181017125013/https://www.rocket.com/common-extensible-cryogenic-engine. [Accessed 29 November 2018].

[35] B. Nufer, "Hypergolic Propellants: The Handling Hazards and Lessons Learned from Use," Kennedy Space Center, NASA, Cape Canaveral, 2010.

[36] NASA, "NASA Tests Engine Technology for Landing Astronauts on the Moon," 14 January 2009. [Online]. Available: https://www.nasa.gov/mission_pages/constellation/news/cece.html. [Accessed 24 March 2019].

[37] B. Leahy, "RL10 Test Paves the Way for Future Starliner Flights," Spaceflight Insider, 19 August 2016. [Online]. Available: https://www.spaceflightinsider.com/organizations/aerojet-rocketdyne/rl10-test-paves-way-future-starliner-flights/.

[38] D. P. Bradley and K. Van Hooser, "Space Shuttle Main Engine - The Relentless Pursuit of Improvement," NASA NTRS, 2011.

[39] G. P. Sutton and O. Biblarz, Rocket Propulsion Elements, Ninth Edition, Wiley, 2016.

[40] J. F. Baumeister, "RL10 Engine Ability to Transition From Atlas to Shuttle/Centaur Program," NASA NTRS, Cleveland, 2015.

[41] H. Kawamoto and T. Miwa, "Mitigation of Lunar Dust Adhered to mechanical Parts of Equipment Used for Lunar Exploration," Journal of Electrostatics, 2011.

[42] Blue Origin, "New Glenn Payload User's Guide," 2018.

[43] T. J. Rudman and K. L. Austad, "The Centaur Upper Stage Vehicle," 2002.

[44] L. D. Kos, T. T. Polsgrove, R. R. Sostaric, E. M. Braden, J. J. Sullivan and T. T. Le, "Altair Descent and Ascent Reference Trajectory Design and Initial Dispersion Analyses," NASA NTRS, 2010.

[45] ISS MCB, "International Deep Space Interoperability Standards," Feburary 2018. [Online]. Available: https://nasasitebuilder-prod-cdn.nasawestprime.com/wp-content/uploads/sites/45/2018/05/03155212/Combined-Draft-C%E2%80%93February-2018.pdf. [Accessed 15 January 2019].

[46] S. F. Balistreri, J. W. Steele, M. E. Caron, Y. J. Laliberte and L. A. Shaw, "International Space Station Common Cabin Air Assembly Condensing Heat Exchanger Hydrophilic Coating Operation, Recovery, and Lessons Learned," NASA, 2013.

[47] A. B. Button and J. J. Sweterlitsch, "Amine Swingbed Payload Testing on ISS," NASA NTRS, 2014.

[48] A. Macatangay and J. Perry, "Cabin Air Quality On Board Mir and the International Space Station--A Comparison," NASA NTRS, 2007.

[49] J. L. Perry, J. H. Agui and R. Vijayakumar, "Submicron and Nanoparticulate Matter Removal by HEPA-Rated Media Filters and Packed Beds of Granular Materials," *NASA NTRS*, 2016.

[50] The Charles Stark Draper Laboratory, "DMS – International Space Station," 2018. [Online]. Available: https://www.draper.com/explore-solutions/dms-international-space-station.

[51] B. D. Gardner, P. M. Ervwin and S. Thoresen, "International Space Station Major Constituent Analyzer On-orbit Performance," NASA, Pomona, California, 2012.

[52] NASA JSC - Advanced Exploration Systems Division, "Logistics Reduction: Universal Waste Management System (LR-UWMS)," 2014. [Online]. Available: https://techport.nasa.gov/view/93128. [Accessed 15 January 2019].

[53] M. Sargusingh, M. S. Anderson, J. L. Broyan, A. V. Macatangay, J. L. Perry, W. F. Schneider, R. L. Gatens and N. Toomariam, "NASA Environmental Control and Life Support Technology Development and Maturation for Exploration: 2017 to 2018 Overview," NASA, Albuquerque, 2018.

[54] NASA, "Human Needs: Sustaining Life During Exploration," NASA, 16 April 2007. [Online]. Available: https://www.nasa.gov/vision/earth/everydaylife/jamestown-needs-fs.html. [Accessed 15 January 2019].

[55] M. S. Anderson, M. K. Ewert and J. F. Keener, "Life Support Baseline Values and Assumptions Document," NASA NTRS, 2015.

[56] K. D. Pickering, "Life Support for Human Spaceflight," National Aeronautics and Space Administration, Houston, 2013.

[57] A. Whitaker, "Overview of ISS US Fire Detection and Suppression System," NASA, Houston, 2003.

[58] S. Editor, "NASA Picks ILC Dover To Build Next-gen Spacesuit," SpaceNews, 26 April 2013. [Online]. Available: https://spacenews.com/35077nasa-picks-ilc-dover-to-build-next-gen-spacesuit/. [Accessed 26 March 2019].

[59] C. Chullen, C. Campbell, W. Paple, S. Murray, R. Wichowski, B. Conger and S. McMillin, "Design and Development Comparison of Rapid Cycle Amine 1.0, 2.0, and 3.0," NASA NTRS, Vienna, 2016.

[60] K. Tate, "NASA's Futuristic Z-2 Spacesuit: How It Works (Infographic)," Space.com, 29 May 2014. [Online]. Available: https://www.space.com/25708-how-nasa-z2-spacesuit-works-infographic.html. [Accessed 26 March 2019].

[61] B. B. Donahue, G. N. Caplin, D. B. Smith, J. Behrens and C. Maulsby, "Lunar Lander Concepts for Human Exploration," *Journal of Spacecraft and Rockets*, vol. 45, no. 2, pp. 383-393, March 2008.

[62] A. Ross, R. Rhodes, D. Graziosi, B. Jones, R. Lee, B. Z. Haque and J. W. G. Jr., "Z-2 Prototype Space Suit Development," in *44th International Conference on Environmental Systems*, Tucson, 2014.

[63] NASA, "NASA Awards Artemis Contract for Lunar Gateway Power, Propulsion | NASA," 23 May 2019. [Online]. Available: https://www.nasa.gov/press-release/nasa-awards-artemis-contract-for-lunar-gateway-power-propulsion. [Accessed 24 May 2019].

[64] NASA, "Piece by Piece: Building Space Launch System's Core Stage," 19 September 2016. [Online]. Available: https://www.nasa.gov/exploration/systems/sls/piece-by-piece-building-sls-core-stage. [Accessed 24 March 2019].

[65] NASA, "European Service Module (ESM) | NASA Glenn Research Center," 7 December 2018. [Online]. Available: https://www1.grc.nasa.gov/space/esm/. [Accessed 24 May 2019].

[66] S. R. Domen, "Emissivity of Aluminized Mylar," Pergamon Press, 1991.

[67] Jet Propulsion Laboratory for Planetary Science Division, "Energy Storage Technologies for Future Planetary Science Missions," NASA, Pasadena, 2017.

[68] Boeing, "Active Thermal Control System (ATCS) Overview".

[69] N. Prasad, S. Trivedi, H. Chen, S. Kutcher, D. Zhang and J. Singh, "Fabrication of Lightweight Radiation Shielding Composite Materials by Field Assisted Sintering Technique (FAST)," NASA NTRS, Hampton, VA, 2017.

[70] JDA Company, "Shipboard furniture catalog," [Online]. Available: https://jdaships.com/pages/sfc#Beds%20and%20berths.

[71] E. Flynn-Evans, K. Gregory, L. Arsintescu and A. Whitmire, "Risk of Performance Decrements and Adverse Health Outcomes Resulting from Sleep Loss, Circadian Desynchronization, and Work Overload," National Aeronautics and Space Administration Lyndon B. Johnson Space Center , Houston, Texas, 2016.

[72] G. C. Brainard and S. W. Lockley, "Testing Solid State Lighting Countermeasures to Improve Circadian Adaptation, Sleep, and Performance During High Fidelity Analog and Flight Studies for the International Space Station (Lighting Effects)," 13 February 2019. [Online]. Available: https://www.nasa.gov/mission_pages/station/research/experiments/2279.html.

[73] D. M. Douglas, T. Swanson, R. Osiander, J. Champion, A. Garrison Darrin, W. Biter and P. Chandrasekhar, "Development of the Variable Emittance Thermal Suite for the Space Technology 5 Microsatellite," NASA, 2001.

[74] J. R. O'Donnell Jr, M. Concha and D. C. Tsai, "Space Technology 5 Launch and Operations," American Astronautical Society, 2007.

[75] "2195 Aluminum Composition Spec," [Online]. Available: http://www.matweb.com/search/datasheet.aspx?matguid=4363dafc7f5545688506d8b4af1e9468. [Accessed 27 March 2019].

[76] "Overview of materials for Epoxy/Carbon Fiber Composite," [Online]. Available: http://www.matweb.com/search/datasheettext.aspx?matguid=39e40851fc164b6c9bda29d798bf3726. [Accessed 27 March 2019].

[77] Spaceflight 101, "Falcon Heavy," Spaceflight 101, 2019. [Online].

[78] Advanced Cooling Technologies, "Spot Cooling Heat Pipes," [Online]. Available: https://www.1-act.com/spot-cooling-heat-pipes/. [Accessed 30 May 2019].

[79] A. Whitaker, "Overview of ISS US Fire Detection and Suppression System," NASA, Houston, 2001.